It follows (because there are two waves traveling in opposite direction for each frequency) that half of the frequencies, those given by (22a), remain unchanged by the interaction. If we denote the roots of (22b) by ω_n' ($n=1, 2, 3, \cdots$), numbered in increasing order, then the quantal energy of the system in its lowest state is given by

$$E'=\hbar\sum_{n=1}^{\infty}(\omega_n'-\omega_n), \tag{23}$$

which has been doubled to take account of the two kinds of polarization.

The question now is whether the series in (23) converges. From (22b) one sees that for large values of ω,

$$\omega_n'-\omega_n\sim\sigma/n\gamma,$$

so that the series in (23) diverges logarithmically. Let us write

$$E'=(\hbar\sigma/\gamma)w, \tag{24}$$

where $w\sim\Sigma(1/n)$. From (17) one then obtains the relation

$$E^2-c^2p^2-m^2c^4=(4\hbar/\gamma)K^2w. \tag{25}$$

Although in the three-dimensional case K was taken as in Eq. (10), in the one-dimensional problem it is better to take

$$K=ce\pi^{\frac{1}{2}}L^{-\frac{1}{2}}S^{-\frac{1}{2}}, \tag{10a}$$

where we think of the electron and field as moving in a (long) cylinder of length L and cross-sectional area S. The right-hand member of (25) becomes $(2e^2\hbar c/S)w$ and one gets, for the positive energy state,

$$E\sim e(2\hbar c/S)^{\frac{1}{4}}w^{\frac{1}{4}}, \tag{26}$$

so that the energy diverges like the square root of a logarithm.

Thus we see that the interaction of the electron with the transverse field gives a divergence in the energy in the one-dimensional case. It is of some interest to note that, if one were using a perturbation calculation based on the assumption that the interaction between electron and field is weak, one would regard the right-hand member of (25) as small; and one would then get, taking $p=0$ for simplicity,

$$E\sim mc^2+(2\hbar K^2/\gamma mc^2)w=mc^2+(e^2\hbar/mcS)w, \tag{27}$$

which in view of the actual logarithmic divergence of w leads to a worse type of infinity than that of Eq. (26).

Although the three-dimensional case is much more complicated and involves features not present in the simple case discussed here, the result obtained in the latter suggests rather strongly that the transverse self-energy of the point electron in the three-dimensional case is inherently divergent.

In conclusion, I should like to express my indebtedness to Professor Wayne A. Bowers for helpful discussions.

PHYSICAL REVIEW VOLUME 87, NUMBER 6 SEPTEMBER 15, 1952

Capture of μ-Mesons in Heavy Elements*

J. W. KEUFFEL, F. B. HARRISON,† T. N. K. GODFREY, AND GEORGE T. REYNOLDS
Palmer Physical Laboratory, Princeton University, Princeton, New Jersey

(Received May 5, 1952)

Measurements have been made of the mean lifetimes of μ-mesons in several heavy elements. Time lags between the arrival of a cosmic-ray meson in the target and its subsequent absorption—as signaled by the neutrons and gamma-rays following capture—are measured using large liquid scintillation counters and a chronotron timing circuit. The timing uncertainty is about 2×10^{-9} sec, and the counting rates are such that a mean life can be determined to an accuracy of 10 percent in about a week's run at sea level. A short-lived component of the decay curves was found and identified as due to neutrons from proton-induced stars. Errors from this effect were avoided. Our latest results for the mean lives, in mμsec, are

Fe 163±27, Hg 58±4, Cu 116±9, Pb 76±4, Sb 99±11, Bi 68±5.

The results are in agreement with the Wheeler Z_{eff}^4 law up through Cu but disagree by a factor 3 for the heavier elements. They are in reasonable agreement with Kennedy's calculations (see following paper). The difference between the mean lives for Hg and Pb is also qualitatively predicted by Kennedy on the basis of a shell model of the nucleus. Our results, together with Kennedy's calculation for Pb, allow us to conclude that the μ-meson-nucleon coupling constant has the same value, within about 25 percent, as recent values of the coupling constants of beta-decay and of the spontaneous disintegration of the μ-meson.

I. INTRODUCTION

IT is now well established that the capture of negative μ-mesons by atomic nuclei is characterized by (1) a weak meson-nucleon coupling and (2) the transfer of most of the meson rest energy following nuclear capture to a light neutral particle.

That the μ-meson interacts weakly with neutrons and protons was convincingly demonstrated by the classic experiment of Conversi, Pancini, and Piccioni.[1]

* Assisted by the joint program of the AEC and ONR.

† Now at Los Alamos Scientific Laboratory, Los Alamos, New Mexico.

[1] Conversi, Pancini, and Piccioni, Phys. Rev. **71**, 209 (1947).

It was shown that negative μ-mesons stopping in condensed matter are not always captured, but that in light elements they decay. Calculations of Fermi and Teller[2] indicated that the time required for a slow meson to come to rest in condensed matter and to fall to the mesonic K-orbit of an atom was less than 10^{-10} sec, a time negligibly short compared with the 2.22-μsec mean life of the meson,[3] and hence entirely too short to explain the fact that negative mesons were not captured in light elements. Thus, the capture probability in light elements was only of the order of the spontaneous decay probability, and this weak interaction ruled out the μ-meson as a possible Yukawa particle.

If a meson in a K-orbit has a chance τ_0^{-1} per second of decaying and a chance Λ of being captured, it will have mean life τ given by $\tau^{-1}=\Lambda+\tau_0^{-1}$. The capture probability Λ may thus be found from a measurement of the mean life in a given element together with the known free decay mean life, τ_0. The mean life is independent of whether one observes decay electrons or any radiation accompanying capture. In a given element, a fraction τ/τ_0 of the mesons will decay. By comparing the yields of decay electrons for mesons stopped in various light elements. Sigurgeirsson and Yamakawa[4] estimated that capture and decay are equally probable in elements of $Z\sim 10$. The capture probabilities for O, NaF, Mg, Al, and S were measured by Ticho,[5] who selected negative mesons by means of a magnetic lens and observed their mean life in absorbers of the various elements. Similar results for Al were reported by Valley.[6] These experiments showed that the capture probability varies approximately as Z^4 and, again, that capture and decay compete on equal terms for $Z\sim 10$.

Besides adding to our knowledge of the strength of the meson-nucleon interaction, μ-meson capture studies may throw light on the question of just what happens to the rest mass of the meson when it disappears. Photographic emulsion work[7,8] and cloud-chamber studies[9,10] have demonstrated the absence of the stars of about 100 Mev which would certainly result if the entire rest energy appeared as nuclear excitation. The basic reaction involved in meson capture is therefore taken to be of the type

$$\mu^-+P\rightarrow N+\nu,$$

where the ν represents a neutrino or a neutral meson. On this picture, most of the rest energy of the μ^--meson is carried away by the light neutral entity. The latter is certainly not a photon, as demonstrated by Piccioni[11] and Chang.[10]

Although a large star will not be produced according to this capture mechanism, the nucleus is expected to receive an excitation of around 15 Mev, according to the calculations of Tiomno and Wheeler.[12] This will generally not suffice to eject a proton, particularly in the heavy nuclei where the Coulomb barrier is important, but one expects on the average one or two neutrons to be boiled off, and the remainder of the energy to appear as gamma-rays of a few Mev or less. We shall call these neutrons and gamma-rays together the meson *capture radiation.*

The above picture is borne out by the experiments of Sard *et al.*,[13] Groetzinger and McClure,[14] and Crouch and Sard,[15] who find that around two neutrons are emitted, on the average, when a μ-meson stops in Pb. These workers used a technique of moderating the neutrons in paraffin and detecting the slow neutrons. The existence of gamma-rays of low energy associated with the stopping of μ-mesons has been demonstrated by Chang,[10] Shanley,[16] and Harris[17] using a cloud chamber. Harris concluded that neither Bohr orbit transitions of the stopping meson nor nuclear transitions following capture were alone sufficient to explain the data.

In an experiment with photographic emulsions exposed below ground, George and Evans[8] found that 8.7 ± 1.7 percent of the μ-mesons captured in the emulsion produced low energy protons, that the average number of prongs per capture was 0.10 ± 0.02, and that the mean number of prongs and the prong distribution suggest that a nuclear excitation of about 15 Mev is produced.

In the experiment to be described, we use the gamma-rays and neutrons following the meson capture event to signal the disappearance of a meson whose time of arrival in the target was previously recorded. In this way we measure the mean life of negative mesons in various elements.

Wheeler[18] has given a theory which predicts that the capture probability is proportional to Z_{eff}^4 ,where Z_{eff} is an effective atomic number introduced to take account of the finite nuclear radius. This correction to Z is less than 10 percent up to $Z=10$, but becomes important for the heavier elements; in Pb, for example, $Z_{\text{eff}}=31.5$. We shall not discuss the theory, as it is reviewed in the following paper by J. M. Kennedy.

One could in principle calculate the constant of proportionality in the Z_{eff}^4 law in terms of the coupling constant g_A involved in the meson-nucleon interaction,

[2] E. Fermi and E. Teller, Phys. Rev. **72**, 399 (1947).
[3] W. E. Bell and E. P. Hincks, Phys. Rev. **84**, 1243 (1951).
[4] T. Sigurgeirsson and A. Yamakawa, Phys. Rev. **71**, 319 (1947).
[5] H. K. Ticho, Phys. Rev. **74**, 1337 (1948).
[6] G. E. Valley, quoted by B. Rossi, *Colston Papers* (Butterworths Scientific Publications, London, 1949), p. 55.
[7] Lattes, Muirhead, Occhialini, and Powell, Nature **159**, 694 (1947).
[8] E. P. George and J. Evans, Proc. Phys. Soc. (London) **64**, 193 (1951).
[9] T. H. Johnson and R. P. Shutt, Phys. Rev. **61**, 380 (1942).
[10] W. Y. Chang, Revs. Modern Phys. **21**, 166 (1949).
[11] O. Piccioni, Phys. Rev. **74**, 1754 (1948).
[12] J. Tiomno and J. A. Wheeler, Revs. Modern Phys. **21**, 153 (1949).
[13] Sard, Ittner, Conforto, and Crouch, Phys. Rev. **74**, 97 (1948).
[14] G. Groetzinger and G. A. McClure, Phys. Rev. **74**, 341 (1948).
[15] M. F. Crouch and R. D. Sard, Phys. Rev. **85**, 120 (1952).
[16] T. J. B. Shanley, Ph.D. thesis, Princeton (1951).
[17] G. G. Harris, Ph.D. thesis, Princeton (1951).
[18] J. A. Wheeler, Revs. Modern Phys. **21**, 133 (1949).

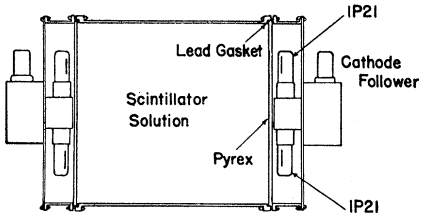

FIG. 1. Plan view of the liquid scintillation counter (S_1) used for the detection of the incident meson. The active volume of solution is 12 in.$\times 11\frac{1}{2}$ in.$\times 1$ in. deep.

and so obtain a value of g_A from the experimental values for the capture probabilities. An order of magnitude calculation of this sort was made by Tiomno and Wheeler,[12] who found that g_A was of the same order as the Fermi constant of β-decay and the constant g_μ of μ-meson decay.

Calculations on the absorption of μ-mesons using a shell model of the nucleus have recently been carried out by Kennedy and are reported in the following paper. From his results, one expects for the heavier elements a less rapid rise in the capture rates with Z than that predicted by the Z_{eff}^4 law. Also, abrupt changes are to be expected in the vicinity of Pb and possibly near the other closed-shell nuclei. Finally, a more accurate calculation of g_A in terms of the absorption rate for Pb is obtained.

A comparison of the theoretical predictions and our experimental values for the capture probabilities is made in a later section of this paper.

II. APPARATUS

A. The Scintillation Counters

The study of the μ-meson capture process has heretofore been limited to elements no heavier than sulfur by two experimental considerations. First, the mean lifetimes become of the same order of magnitude as the random lags of the Geiger counters which have until now been used. Second, the inefficiency of the Geiger counters for low energy gamma-rays and neutrons has made it necessary to measure the lifetimes by means of the decay electrons of those mesons which escape capture; since in the heavy elements the fraction of mesons escaping capture is small, the rates become prohibitively low.

The discovery of the liquid scintillation counter[19,20] and the subsequent development of a large-area version of this type of counter[21] made available an ideal detector for the meson capture experiments. The combination of large area, good efficiencies for the detection of both gamma-rays and neutrons in the Mev range, and fast pulses resulted in a successful technique for the measurement of mean life using sea-level mesons.

Two types of liquid scintillation counters were used. For the principles involved in their design, the reader is referred to the paper by Harrison.[21] A plan view of the first type—used for the detection of ionizing particles (the incident mesons) over a wide area—is shown in Fig. 1. The section containing the liquid was one inch deep, and 12 inches by $11\frac{1}{2}$ inches in area. The scintillating material was a solution of terphenyl in toluene, 3.5 grams per liter. The windows were of one-eighth inch Pyrex, and a rough measurement showed that they absorb only a few percent of the light from the scintillations. The lead gaskets used to seal the windows have been very satisfactory; there have been no signs of leakage, and no windows were broken in assembly after the bearing surfaces were made properly flat. The tank was lined with a thin sheet of aluminum to reflect the light. The walls were made thin so as to reduce the amount of extraneous material to a minimum. There was a total of 1.75 g/cm^2 of copper and 0.25 g/cm^2 of aluminum above and below the liquid.

Four type 1P21 photomultipliers were used. They were selected for low noise background. The voltages on the dynodes of these tubes were adjusted so as to match the tubes for response to a given amount of light. The anodes of each pair of tubes were connected together and fed into a cathode follower, and the cathode followers were fed in parallel into the input of a fast amplifier. The efficiency of this type of counter for the detection of minimum ionizing particles averaged over the surface of the counter was about 65 percent when the counter was operated at a discriminator level such that the noise rate was 300 sec^{-1}.

The second type of scintillation counter (see Fig. 2) was designed for the detection of the meson capture radiation. Somewhat better light collection than in the first type of counter was achieved without very much reduction in sensitive volume by using type 5819 end-window photomultipliers mounted one at each end of a rectangular tube 3 inches square and one foot long. The efficiency of this counter for mesons was very nearly 100 percent, but the situation with regard to gamma-rays and neutrons is much more complicated. Both the chance that a photon or neutron will make a recoil particle, and the chance that the flash produced by the ionizing recoil will be detected, depend sensitively on the energy distribution of the capture radiation, and this is not known. As an order of magnitude, one may take perhaps 10 percent as the over-all efficiency for each type of radiation. A knowledge of the efficiency is fortunately not necessary in the present form of the experiment.

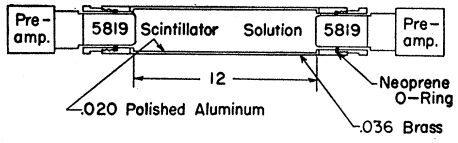

FIG. 2. Plan view of the liquid scintillation counter S_2 used for the detection of the capture radiation. The active volume of solution is 3 in.$\times 3$ in.$\times 12$ in.

[19] Reynolds, Harrison, and Salvini, Phys. Rev. **78**, 488 (1950).
[20] H. Kallmann, Phys. Rev. **78**, 621 (1950).
[21] F. B. Harrison, Nucleonics (to be published).

The four type 5819 photomultipliers used so far lasted for only $2\frac{1}{2}$ to $3\frac{1}{2}$ months of continuous operation. The over-all voltage applied to the tubes was about 800 volts and was held in each case to ± 2 volts. The sensitivity of each tube decreased gradually during the last month of its life and then faded out rapidly in a few days. The cathodes were at a negative high potential, and they were separated only by the glass envelope of the tube from the liquid scintillator which was at ground potential. The instability and short life of the 5819's may be peculiar to operation under the conditions described and not typical of normal 5819 behavior. The possibility that the close proximity of the grounded liquid to the cathode was the cause of the failure of the tubes is being investigated.

B. Counter Arrangement

The disposition of the counters and target is shown in Fig. 3. Whenever there was a "coarse" coincidence between the top tray "A" of Geiger counters, the scintillator S_1, and the scintillator S_2, but no count from the anticoincidence bank of Geiger counters "X," the timing circuit discussed below made a photographic record of the time interval between the pulses from S_1 and S_2. The system was designed to select negative cosmic-ray mesons which stop in the target, and there produce a non-ionizing radiation which crosses the top tray of the anticoincidence bank "X" and is detected in S_2. The mean life of negative mesons in the element used as target was then obtained from the distribution of the time delays of S_2 relative to S_1. The resolving time for the selection of events was longer than these delays, of course.

The present method of selecting stopped negative mesons, based on the requirement of a non-ionizing link, has the advantage over a selection system using a magnetic lens in that it accepts a very much larger cone of mesons incident upon the target. The question of how well the system discriminates against other types of events is discussed in Sec. IV.

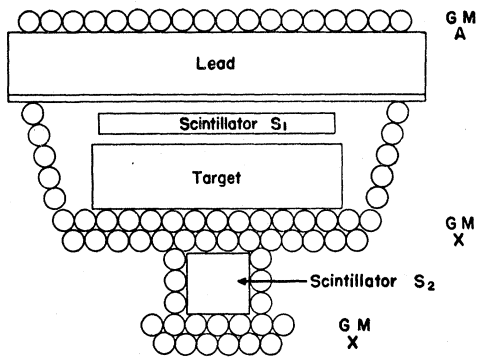

FIG. 3. Experimental disposition. All the G-M counters are 1 in. in diameter. The dimensions normal to the plane of the figure of the G-M counter bank "A," the Pb electron filter, the two scintillation counters, and the target are all 12 in. The 58 counters of the anticoincidence bank "X" have a 23-in. sensitive length.

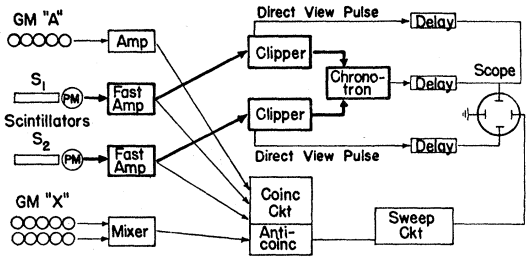

FIG. 4. Block diagram of the electronic apparatus. The coincidence circuit selects events where pulses from A, S_1, and S_2 coincide to within a few μsec, but there is no pulse from X. The precise time interval between S_1 and S_2 is measured by the chronotron. Pulses from the photomultipliers are amplified using Hewlett-Packard 460-A and 460-B distributed amplifiers, then shaped in the clippers and sent to the chronotron line. "Fast" portions of the circuit are shown in heavy black lines. The rise-time at the clipper input is about 5 mμsec. The scintillator pulses are also delayed and directly presented on the scope trace ("direct view" lines).

The targets have been approximately 10-cm thick and 30 cm$\times$30 cm in area. Since a gamma-ray has an absorption free path of only about 2 cm in a heavy element, even at the minimum of the absorption curve, such thick targets would not be worthwhile were it not for the neutrons of the capture radiation. These neutrons undergo principally elastic scattering which does not appreciably diminish the source strength. It will be shown later that most of our counts come from neutrons. The thick target is therefore definitely advantageous from the rate standpoint. For elements which are not available in large quantities, however, it is anticipated that dispositions involving smaller targets and larger, more efficient scintillators placed closer to the target will be employed.

C. Event Selector Circuits

The electronic equipment falls into two main divisions: the selector circuits and the timing circuit. Figure 4 shows a block diagram of the complete set-up. We shall first discuss the system that selects the stopped-meson events and actuates the camera.

Pulses from the counters go to a coincidence circuit of conventional design, whose output triggers the oscilloscope sweep circuit. A camera with the shutter continuously open views the scope screen; the oscilloscope beam is normally off, but is turned on by the sweep circuit, and a photograph is made of the trace associated with the desired coincidence. A univibrator-controlled motor then advances the 35-mm Linagraph Ortho film about 2.5 mm in readiness for the next event.

It is essential that the coincidence circuit response be independent of the delay of S_2 relative to S_1, over the range of time intervals dealt with. As will be seen later, this range was from -1.0 to $+1.5$ μsec. The pulse widths of the univibrators in each coincidence channel were carefully adjusted to give a range of at least -2.0 to $+3.5$ μsec, and the resolving time limits were experimentally checked using known delay lines.

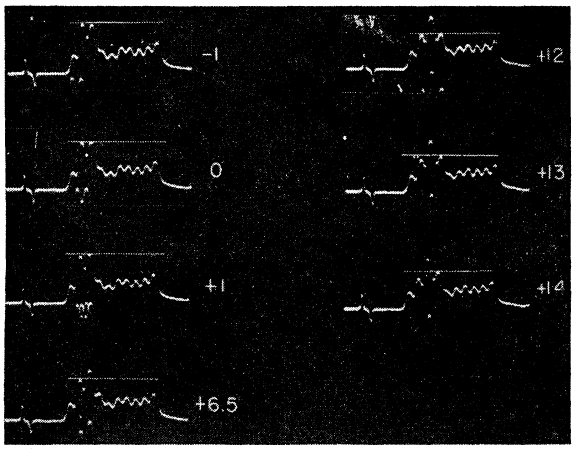

FIG. 5. Photographs of oscilloscope traces obtained using a pair of test pulses from a mercury-switch pulser. The sweep starts after 1.8 μsec. Then, left to right, we have the direct pulse from S_1, delayed 2.6 μsec; the direct S_2, delayed 3.0 μsec; and the chronotron superposition locus, with first detector pulse delayed 4.7 μsec. On the trace labeled "0" the test pulses met on the chronotron line midway between the second and third detectors, since the second and third detector pulses are up, and are just equal. The numbers opposite the other traces indicate the number of feet of Rg-7-U cable inserted between the pulse and the S_2 input of the chronotron; 1 ft = 1.225 mμsec. The zero setting of the chronotron can be shifted at will, of course, by inserting cable in one side.

The univibrator pulse width in the anticoincidence channel was made amply wide to overlap any possible coincidence combination. To allow for time lags in the firing of the anticoincidence counters, the pulse from S_1 was delayed 1.0 μsec before going into the coincidence circuit. Then if A, S_1, and S_2 were tripped simultaneously, a coincidence was not formed until the X bank had had a microsecond to signal an anticoincidence. The output of the X-bank mixer was also fed directly to the blanker input of the sweep circuit; in this way, part at least of the trace was blanked if any of the anticoincidence counters fired at any time during the trace. We rejected such traces, thus making our anticoincidence system independent of the time of firing of the X counters up to 10 μsec or more. The blanker also provided a constant check on the operation of the anticoincidence system generally.

The pulses from the two scintillation counter amplifiers were broadened before going into the coincidence circuit, in order to stabilize the triggering thresholds of the univibrators in each coincidence channel; these univibrators set the level at which scintillator pulses were accepted.

D. Timing Circuits

For each event that triggers the selector circuit, we wish to know the time interval between the pulse from S_1 (the arriving meson) and the pulse from S_2 (the radiation signaling the meson capture). The measurement is carried out with a chronotron-type timing circuit similar to the one described by Keuffel.[22] The pulses from each scintillation counter are amplified (see Fig. 4) and sent to a "clipper," whose function is to limit them in size and duration. A uniform pulse about 10 volts high and 25 mμsec wide at half-maximum emerges from each clipper; these pulses are applied, one to each end of a length of 100-ohm coaxial cable. The basic "chronotron" principle is to determine the time interval between the two pulses by observing the point at which they meet. Thus, for example, if the pulses are applied simultaneously to the ends of the line, they will evidently meet in the middle, while if one pulse is delayed with respect to the other, the meeting point will be shifted towards the side of the later pulse. The time interval between the two pulses is given by $2x/c$, where x is the displacement of the meeting point from the center and c is the velocity of propagation of the pulses.

The meeting point of the pulses is ascertained by means of 10 crystal diode detectors spaced along the cable at 16-mμsec intervals.[23] The output of each detector unit is a rounded pulse about 0.5 μsec wide, whose amplitude is proportional to the peak voltage at that point along the line. A plot of the detector outputs against the detector positions is called a *superposition locus*, and the maximum of this locus tells us the meeting point of the pulses. In order to record the superposition locus, each detector output pulse is passed through a delay line, amplified, and presented on the oscilloscope trace. By delaying the first detector pulse 4.7 μsec, the second 5.2 μsec, the third 5.7 μsec, and so on, the pulses are made to appear in order on the later part of the trace, leaving the first portion of the trace available for other purposes. Since the detector output pulses are rather slow, they may be delayed without much dispersion. The attenuation in each delay line is compensated by a potentiometer adjustment. The delay-line outputs are mixed before amplification, so that the relative gains depend primarily on the stability of the 1N34 crystals in the detectors and in the mixer.

Some photographs of oscilloscope traces are shown in Fig. 5. From the superposition locus it is possible to tell at a glance between which two detectors the pulses met and to which of these two detectors the meeting was closest. This gives us 18 chronotron channels; the ones at each end are not used, leaving 16 channels or a range of 256 mμsec for delay measurements.

The chronotron measures delays in the range 0 to 256 mμsec with a precision of about 2 mμsec. In addition, a coarse timing range which measures delays between -1.0 μsec and $+1.5$ μsec with a precision of perhaps 15 mμsec is provided by presenting the pulses from the two scintillators, suitably delayed, on the

[22] J. W. Keuffel, Rev. Sci. Instr. **20**, 197 (1949).

[23] The 16-mμsec detector spacing proved adequate for the mean lives measured so far, although a 6-mμsec interval between detectors was used for investigating the neutrons from proton-induced stars.

oscilloscope screen in the conventional manner. These "direct view" pulses may be seen at the beginning of the traces in Fig. 5.

At first sight it might seem that the chronotron is unnecessarily complicated compared to the direct presentation of the fast pulses on a scope sweep, but it has several important advantages. The provision of a fine and a coarse timing range on a single oscilloscope sweep is one such advantage. Another is that the chronotron permits the recording of the time delay to be postponed several μsec while the coincidence circuit —which involves slow Geiger counters—is making up its mind to accept or reject the event; fast pulses cannot be delayed without dispersion in presently available cables, but the slow chronotron detector pulses can be delayed. Also, the chronotron trace is easy to photograph, since the sweep speed is moderate (1.33 μsec/cm). Finally, the data can be read easily from the film. The delays are to be grouped in any case, and one can tell rapidly to which of the 16 channels a lag is to be assigned. The ease of reading is particularly important since a large percentage of the events selected and photographed show no appreciable lag (shower events, etc.), and these can be run through rapidly and reliably.

The chronotron may be regarded as a multichannel time discriminator, and as in every multichannel discriminator, the stability of the channel boundaries is a problem. We calibrated the instrument by feeding both fast amplifiers from a mercury-switch pulser whose output was shaped to simulate a scintillation pulse. Cable was inserted between the pulser and the S_2 amplifier input to shift the superposition locus. The time delay of the cable required to shift the locus to each channel boundary was measured using a crystal-calibrated oscillator. The channel boundaries (with 16 mμsec channels) were found to deviate randomly from their correct positions by about 2 mμsec. These deviations were due to several small effects, many of which we hope to eliminate in the future. In any case the boundary errors throw counts from one channel to an adjacent one but no counts are missed.

E. Over-all Timing Precision

In addition to the chronotron errors discussed above, errors are caused by fluctuations in the time lag between the passage of the particle through the counter and the arrival of a pulse at the chronotron. The random counter lags were studied as follows: Fast mesons passing through both scintillation counters were selected by requiring a coincidence AS_1S_2X, and the time lags between S_1 and S_2 were measured for each event. The distribution of these lags was roughly Gaussian in shape, with a standard deviation of 1.5 mμsec. Although it was not possible to check the shape of the curve accurately with the large chronotron channel width used (6 mμsec), the number of lags that fell outside of ± 6 mμsec was 0.1 percent or less.

During the timing uncertainty measurement, a 20-db attenuator was placed in the S_2 amplifier input to reduce the large meson pulses to a size comparable to the distribution of pulses produced by meson capture events. We also measured the relative lags between the pulses from the photomultipliers at each end of S_2 when gamma-rays were being counted; even with this stringent method the standard deviation was only about 2.5 mμsec.

It will be seen that time lag uncertainties as small as these introduce a negligible error in our results.

III. EXPERIMENTAL PROCEDURE

A. Scintillation Counter Settings

The initial adjustment in setting up the apparatus for a run was to set the level at which scintillation counter pulses were accepted. Using the mercury-switch pulser, we first determined the pulse required at the amplifier input to cut off the limiter tube in the clipper. The coincidence circuit sensitivity for that channel was then adjusted so that it would accept only pulses larger than this value. In this way we made sure that for any event accepted by the selector circuits, the scintillation pulse was big enough to actuate the chronotron properly. Next, the photomultiplier voltages were adjusted until the total noise rate accepted from each scintillation counter was about 300 sec^{-1}. The coincidence rates (S_1X) and (S_2X) were then measured, the latter with a standard 20-db attenuator in the S_2 amplifier input. These rates were taken as a measure of the over-all efficiency of each scintillator, since they represent the efficiency of the scintillators for counting a certain flux of ionizing cosmic rays. The purpose of the attenuator was to make the efficiency of S_2 more sensitive to the level of pulse heights accepted by the apparatus. Once the (S_1X) and (S_2X) rates had been measured, they were held constant to about 10 percent during a run, and as nearly as possible from one run to the next, by adjusting the photomultiplier voltages. As far as the mean life measurements are concerned, of course, rate stability is not necessary, but it is desirable as an over-all check on the apparatus. Rates were checked daily, and the only serious drift was in the sensitivity of the 5819 photomultipliers, as mentioned earlier.

B. Chronotron Adjustments

The potentiometers in each chronotron detector circuit were first adjusted so that, with a standard test pulse applied to each detector in turn, the corresponding pulses on the superposition locus were identical. Crystal characteristics vary from one crystal to another, but are quite stable with respect to time; it was necessary to equalize the detectors at a level corresponding to two clipper pulses meeting at or near the detector, but once so adjusted, their stability was excellent and a monthly readjustment more than adequate.

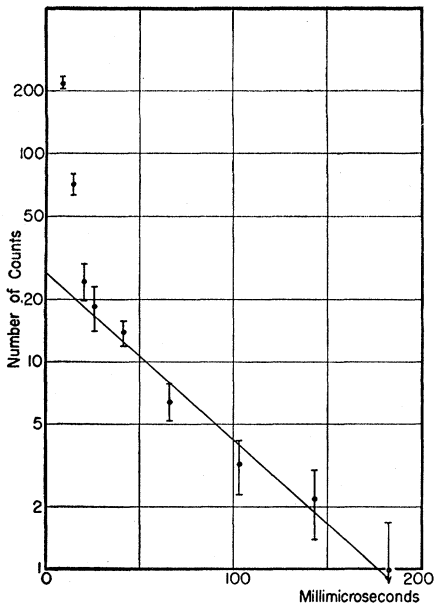

FIG. 6. Typical differential distribution of delayed counts in S_2, obtained with high time resolution (6 mμsec chronotron channel width). Each point represents the total number of counts in 72 hours of counting per 6 mμsec of delay. The short-lived component is due to proton-induced stars and the long component to μ-meson capture. Small backgrounds due to noise and positive meson decay have been subtracted. Disposition: Hg target, thickness 136 g/cm^2, no Pb filter above S_1.

The variations in photoelectron transit time from one photomultiplier to another are negligible for the 1P21 tubes. The 5819's, however, were individually matched (a matter of 2 or 3 ft of cable) and the chronotron "zeroed" as follows: Fast mesons passing through both scintillators were selected using the coincidence circuit, and the time delays between S_1 and S_2 were measured. The lengths of cable from the 5819's to the S_2 amplifier, and from the S_1 clipper to the chronotron, were then adjusted so that the center of the relative delay distribution lay at the boundary between the first two chronotron channels. During this adjustment a 20-db attenuator was inserted at the S_2 input, in order to make the pulse-height distribution from the mesons more nearly like the pulses from the capture radiation.

In order to minimize channel boundary errors, the zero of the chronotron was rotated regularly, during a run, over four different channel boundaries—two at one end of the chronotron and two at the other with the instrument switched end-for-end. After each switch, the zero was checked by observing straight-through mesons in the manner just described.

Accurate knowledge of the oscilloscope sweep speed is necessary for measuring lags longer than the range of the chronotron. We calibrated the sweep by photographing a 2-Mc/sec signal from a crystal-controlled oscillator.

Apart from the rate adjustments, chronotron zero rotation and trace calibrations, the apparatus ran automatically on a 24-hour basis. There were very few failures, and almost all failures showed up immediately on the oscilloscope pictures. The continuous check made possible by the oscilloscope photographs greatly increased our confidence in the data.

IV. ANALYSIS OF THE PICTURES

Approximately 10 percent of the pictures show lags that could be interpreted as μ-meson captures. This is to be expected since the selection of events by the coincidence circuit is purposely made very loose with respect to time delays between S_1 and S_2. The detailed classification of events according to time delays is carried out with the aid of the pictures. This procedure removes much of the "blindness" of cosmic-ray counting experiments. It enables us to identify effects due to components other than μ-mesons and to correct for them if need be. In this section the time delay analysis of the pictures is discussed in terms of the various cosmic-ray components, and the procedure outlined by which the mean lives are obtained.

A. Zero Lag Events: Soft Component

We call a picture showing a lag in either of the two chronotron channels adjacent to the zero of time a "zero lag." Some 70 percent of the pictures fall in this category, and they are due to a number of causes. The soft component may produce the right combination of electrons in A and S_1, plus a photon that crosses the anticoincidence counters and is detected in S_2. A fast meson may be recorded due to anticoincidence inefficiency. Or the gamma-radiation from the Bohr-orbit transitions of a stopped meson may be detected. A considerable number of zero lag pictures also come from the nuclear events discussed below. Since the random delay errors of the scintillation counters are very small, the zero lag events cause no trouble except to increase the number of pictures that must be scanned and rejected.

B. Very Short Lags and the Nuclear Component

At first sight one would not expect the nuclear component to produce delayed events. Decays from π-mesons locally produced by the nuclear component are ruled out by the requirement of a non-ionizing link and by the very short μ-meson range. In a preliminary series of experiments, however, the decay curves for Bi, Pb, Hg, and Fe were examined with the chronotron detector spacings set up to give 6 mμsec channels. The delay distributions exhibited in all four cases two components, one with a mean life at least 10 times shorter than the other. Figure 6 shows a typical curve. We have identified the short component with events where a proton of some hundreds of Mev triggers A and S_1, and makes a nuclear interaction either in the target or the Pb above it; an evaporation neutron of a few Mev then crosses the anticoincidence bank of counters and is

recorded, with a delay due to its time of flight, in S_2. If the nuclear interaction is in the Pb above S_1, there must, of course, be either an ionizing secondary or another neutron which triggers S_1; but in either case the event must not be so violent as to produce penetrating secondaries which would discharge the anticoincidence counters.

An estimate of the frequency of such nuclear events relative to the rate of μ-meson absorption events may be made from photographic emulsion data.[24] The rate of proton-induced stars of three or more prongs, multiplied by 2 (as a guess) to include events with 2, 1, or zero prongs, and divided by 12 to get from mountain altitudes to sea level, is about 4 kg^{-1} hr^{-1}. For the rate of stopped negative μ-mesons in our apparatus (effective solid angle ~ 1) we obtain from Rossi's differential range spectrum[25] the value 5 kg^{-1} hr^{-1}. The mean multiplicity of neutrons from proton-induced stars is not known, but for the roughly similar stars produced in Pb by negative π-mesons, Tongiorgi and Edwards[26] find a value ~ 7. The multiplicity from μ-capture found by Sard is ~ 2. Since the chance of detecting a given event in our apparatus is small, the observed rates should be proportional to the neutron multiplicities. We assume that a neutron from a star has about the same chance of being detected in S_2 as a μ-meson produced neutron, in spite of different energy distributions; this may not be too bad an assumption as most of the neutrons probably have an energy of a few Mev for both types of events, and the lower cross section of the high energy neutrons is compensated by the larger scintillations they produce. We should therefore expect to see roughly three times as many nuclear events as meson absorptions.

This ratio is to be compared with the ratio 4:1 between the total numbers of counts in each of the two components of Fig. 6. The data were taken with no Pb filter above S_1, so that the short component would come from stars produced in the target only. Both components were assumed to follow exponential decays in deducing the ratio of counts in each. Since it is impossible to distinguish the short component from the "zero lag" events in the first chronotron channel (0 to 6 mμsec), an extrapolation was necessary.

In view of the large uncertainties of the calculation, the close agreement of the short component rate with that predicted by the proton-induced star hypothesis must be considered fortuitous.

The exponential nature of the short delay component may be understood on the basis of a sort of diffusion of the neutrons. Their mean free path is about 5 cm, and before emerging they are likely to make a small number of elastic collisions with the heavy nuclei. The mean life of the exponential is 4 mμsec, which is about the time it takes a 3-Mev neutron to go 10 cm.

To test our hypothesis further as to the identity of the short component, we performed a series of auxiliary experiments. It was first established that the mean life of the long component varied with atomic number, while the short component exhibited no very strong Z dependence. Next, we varied the thickness of the Pb filter above S_1 from 0 to 8 in., and found that the intensity and mean life of the long component changed very little, as would be expected from the flat μ-meson range spectrum. On the other hand, as the thickness of Pb increased the over-all rate of lags in the 0–30 mμsec region decreased, but there was an increase in the number of lags in the 18–30 mμsec region. Since many protons will interact or stop in the filter, we should expect a decrease in the number of stars in the target, and hence fewer short lags, but an increase in lags corresponding to stars produced in the filter. Neutrons from the filter must diffuse a longer distance than neutrons from the target, and hence would appear in the later region.

In a further attempt to verify that protons were indeed responsible for the short component, a 34 g/cm^2 layer of carbon was placed above the apparatus. According to the results of Ballam,[27] the number of protons produced in a 44 g/cm^2 layer of carbon by neutrons is comparable to the number originally present in the cosmic-ray beam at sea level. A large auxiliary Geiger counter tray was placed above the carbon and connected to a neon bulb, which was photographed along with the trace. We found that for the short component, 25 percent of the incident rays were non-ionizing as they entered the carbon generating layer; whereas the primaries of the long component were all ionizing except for a small fraction attributable to the inefficiency of the Geiger tray.

As a result of the foregoing calculations and experiments, we conclude (1) that the long component is due to μ-mesons, (2) that most—and probably all—of the short component is due to proton-induced stars. We think it unlikely that some other process, as, for example, the neutrons accompanying extensive air showers, plays much of a role.

Whatever the origin of the short component, it can be eliminated from our experiment by starting to count μ-mesons only after a sufficiently long time, and by using as thin a Pb filter as possible. For the mean life measurements reported here, we started to count only after 32 mμsec, a comfortable margin. The short component caused a large error in our previously reported result for Sb,[28] although the earlier value for Cu was not much affected.

[24] Brown, Camerini, Fowler, Heitler, King, and Powell, Phil. Mag. **40**, 862 (1949).
[25] B. Rossi, Revs. Modern Phys. **20**, 537 (1948).
[26] V. Cocconi-Tongiorgi and D. A. Edwards, Bull. Am. Phys. Soc. **27**, No. 3, 44 (1952).
[27] J. Ballam (to be published).
[28] Harrison, Keuffel, and Reynolds, Phys. Rev. **83**, 680 (1951).

TABLE I. Typical counting rates.

Target		100 kg Pb
Running time		165 hours
Total pictures		5100
μ^- events (lags between 32 and 256 mμsec)		507
μ^+ background (spread out over 2 μsec)		500
Noise (lags between -1.0 and $+2.5$ μsec)		450
Zero lags (showers, nuclear component, etc.)		3650
Counts in first useful channel (32 to 48 mμsec):		
μ^-	115	
μ^+ background	3.8	
Noise background	1.2	
Ratio, μ^- to background	23	

C. Positive Mesons and Random Noise

The remaining 20 percent of the pictures show lags of the order of 1 or 2 μsec, and some of the lags are negative, that is, S_2 fired before S_1. The negative lags, and some of the positive lags, are due to a noise pulse from S_2, combining with either an accidental or a real coincidence between A and S_1; the real coincidences are the most numerous. The random noise background rate for positive lags is found from the rate of negative lag pictures.

When the noise background has been subtracted from the long positive lags, it is found that the remaining lags show a distribution that is consistent with the 2.22-μsec mean life of the positive μ-meson. These pictures are assumed to be due to positive mesons that stop in the target and decay; the decay positron has scant chance of emerging from the target, but is almost certain to radiate, and will in any case annihilate, producing a gamma-ray which may cross the anticoincidence bank and be detected in S_2. The positive meson background in the region of short delays is found by extrapolation, using the number of lags between 0.5 and 1.5 μsec and the 2.22-μsec mean life.

Despite the fact that the total number of background counts is comparable to the useful μ^- rate, the background is not serious as it is spread out over a delay range 10 to 20 times longer than typical negative meson mean lives for elements with $Z \geq 30$. The background is the factor limiting the application of the present form of the experiment to lighter elements.

D. Satellite Pulses from Photomultipliers

In the course of the experiment it was noticed that there was sometimes a second pulse from one of the scintillators, even when we selected events where only one particle, a fast meson, had passed through the tank. These pulses occurred in both tanks, and had time delays of the order of a microsecond. An investigation of the effect showed that the satellite pulses are a photomultiplier effect and do not come from the phosphor. The investigation has been previously reported.[29]

The presence of these delayed pulses made it necessary to count only the first pulse from either tank. So long as this is done—and it was always possible to do so—the satellite pulses introduce no error.

V. RESULTS

Counting rates for a typical 8-day run are presented in Table I. The μ^- rate agrees with the value to be expected from Rossi's meson range spectrum[25] if we take the efficiency of S_2 for neutrons as 30 percent. This value seems high, but there are uncertainties of perhaps a factor 2 in the calculation. Figure 7 shows a differential decay curve for one of two runs taken with Hg as the target. The noise and positive meson backgrounds, which amounted to approximately 1/20 the counting rate in the first chronotron channel, have been subtracted. This run represents about 450 counts, approximately half of our data for Hg. The mean lives are determined by the method of Peierls,[30] and the line shown on the graph was drawn using the slope and intercept obtained from the Peierls analysis of the data for that run.

Figure 8 shows a similar plot for Pb, in this case representing some 950 counts. A summary of individual runs and the weighted means for each of six elements is given in Table II.

The errors quoted are the statistical errors obtained by the Peierls method. In each case the relative standard error is given by $(\sigma/M)^{\frac{1}{2}}$, where σ is a constant that depends upon the counting-rate-to-background ratio, but is usually about 3, and M is the net number of counts observed. According to Peierls, it is worthwhile to count delays up to three or four mean lives; there is a broad optimum in the maximum value of delay to be taken, which depends on the background.

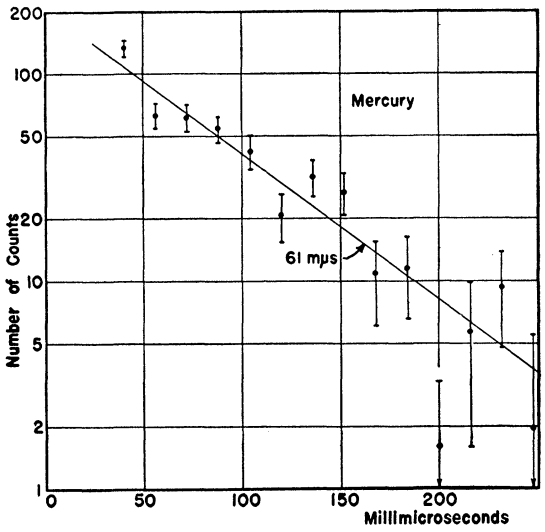

FIG. 7. Differential decay curve for one of two runs with Hg target. The total number of counts was 450. The slope and intercept of the line were drawn according to the Peierls analysis for this run. The flags shown are statistical. Chronotron channel boundary errors, which throw counts from one channel into an adjacent one but do not much affect the mean life, are also present.

[29] Godfrey, Harrison, and Keuffel, Phys. Rev. 84, 1248 (1951).

[30] R. Peierls, Proc. Roy. Soc. (London) A149, 467 (1935).

The individual points of the differential decay curves show fluctuations about the lines larger than one should expect on the basis of the flags shown, which are the usual statistical ones. These additional fluctuations are attributed to chronotron channel boundary errors, which are expected to amount to 1 or 2 mμsec for each boundary, or perhaps 2 or 3 mμsec out of 16 mμsec for the width of a channel. We believe channel width errors of this magnitude suffice to account for the observed fluctuations. The channel boundary errors have a very much worse effect on the appearance of the differential decay curves than they do on the mean lives because counts thrown out of one channel are not lost, but appear in the adjacent channel, and the magnitudes of the boundary shifts are small compared to the mean lives measured. It is hard to estimate the effect quantitatively, but we believe the absolute error from this source can hardly exceed 5 percent in the worst case, that of Hg. The relative error from one element to the next should be negligible in comparison to the statistical errors.

The internal consistency of the data as shown by the agreement between the various runs in Table II is quite satisfactory, lending support to the correctness of the statistical analysis.

It has so far been assumed that the time lag between the capture of a meson and the chronotron pulse resulting therefrom is negligible. As pointed out by Rossi,[31] timing errors will not affect the shape of the decay curve provided (*a*) that the time lag error distribution is independent of the true delay, and (*b*) that one does not start counting until a time greater than the largest error expected. In the case of the random time-lag uncertainties of the scintillation counters, which are less than 2 mμsec, the conditions are certainly satisfied; we do not start counting until 32 mμsec. It is possible, however, that lags may occur between the capture of the meson and the scintillation in S_2 owing to two effects: time of flight of the neutrons and isomeric transitions of the gamma-rays.

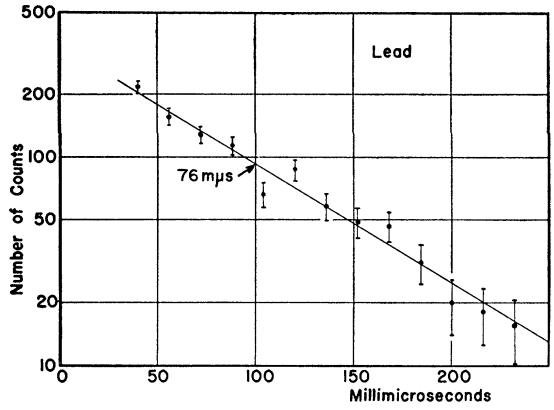

FIG. 8. Differential delay curve similar to Fig. 7 for Pb. A total of 950 counts are represented.

[31] B. Rossi and N. Nereson, Phys. Rev. **62**, 417 (1942).

TABLE II. Summary of mean lives.

Element	Z	Z_{eff}[a]	Mean life (mμsec) Individual runs	Weighted mean	Accuracy %
Fe	26	19.5	161±30 171±60	163±27	17
Cu	29	20.6	117±14 95±18 122±14[b]	116±9	7.5
Sb	51	27.2	105±12 92±12 (50±6)[b]	99±11	11
Hg	80	31.2	54±5 61±5	58±4	6.5
Pb	82	31.4	73±10 73±6 80±6	76±4	5
Bi	83	31.5	63±8 72±7	68±5	8

[a] From Wheeler (see reference 18).
[b] Previously published result (see reference 28). The early Sb value was strongly affected by nuclear events and is not included in the mean.

Before discussing these effects we shall describe an auxiliary measurement which shows that our counts are due almost entirely to neutrons. A comparison was made for Pb and for Cu between the meson capture rate with a 10-cm target and with a 2.5-cm target, other conditions remaining the same. We found that after solid angle corrections had been made, the thin target gave about one-fourth as many counts as the thick one for both elements. The result is consistent with the behavior of neutrons; the stopping mesons provide a diffuse, reasonably uniform source and the elastic scattering does not much affect the counting rate. On the other hand, practically all the gamma-rays, if any, would come from the 2.5 cm closest to S_2 because of absorption. From our measurements we believe that about one-eighth of the counts from the usual 10-cm target are due to gamma-rays.

Time lags from isomeric transitions following capture can therefore be ruled out. For not only are gamma-rays scarce, but in addition, most nuclei with a few Mev excitation are expected to find their way promptly to the ground state. It should also be remembered that even if the capturing nucleus has but a single isotope, the residual nuclei which radiate will consist of a number of isotopes corresponding to the parent nucleus less 0, 1, 2, or even 3 neutrons. No single isomeric level could predominate. Finally, most isomeric gamma-rays are of low energy and very strongly absorbed.

Time lags due to neutron time-of-flight are certainly present. Such lags, however, are independent of the delay between the arrival of the meson and its capture. Consequently, the shape of the decay curve will be unaffected provided we start counting at a time greater than the largest expected time-of-flight. Now the problem of neutron time-of-flight has already been discussed in connection with the neutrons from proton-induced stars; by accepting only counts delayed more than 32 mμsec we eliminate both of these effects. While the mean neutron energy will be somewhat less for

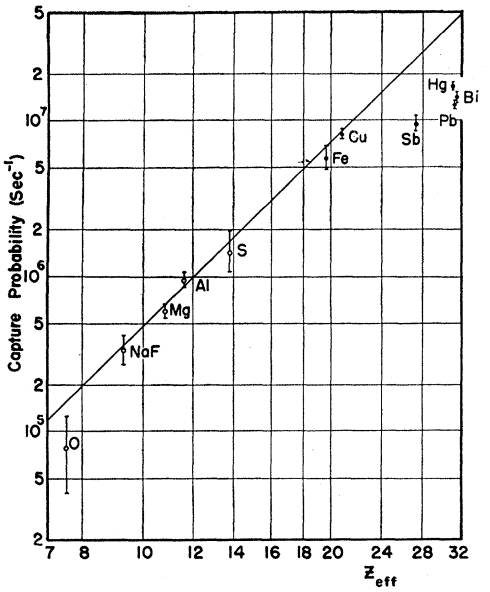

FIG. 9. Capture probabilities *vs* Z_{eff} of Wheeler Theory. Points shown in circles are the results of Ticho. Our results are shown as solid dots. A line with a slope corresponding to the Z_{eff}^4 law has been fitted to the elements up through Cu.

neutrons from meson capture than from stars, and hence the time lags greater, the diffusion mean life for the star-induced neutrons was only 4 mμsec. The 32-mμsec margin is obviously ample.

The effect of extraneous materials in the target region (Fe supports and Cu counter walls) on the measured mean lives is estimated to be less than 1 percent.

The capture probabilities computed from our results for the mean lives are plotted in Fig. 9 against the Z_{eff} of Wheeler. Previous results of Ticho[5] and Valley[6] for the light elements are also shown. The straight line is a fourth-power law fitted to the elements up through Cu.

It is seen that the Z_{eff}^4 law is in agreement with experiment over a considerable range, but that the capture probabilities for the heavier elements fall below the curve by approximately a factor three.

In the following paper Kennedy calculates the capture probabilities for Ca and for Pb, using a shell model of the nucleus. He finds for the ratio of these probabilities the value 6.1. Although we have not yet measured the capture rate for Ca ($Z_{\text{eff}}=16.1$), it probably does not lie far from the line drawn through the neighboring elements. Taking the value for Ca from the line, we find the ratio to be 4.3. If the capture probability for Ca falls below the line because of the closed-shell character of the Ca nucleus, the ratio will be larger. The agreement is thus satisfactory, considering the present incompleteness of the theory and the experimental uncertainties.

In Fig. 10 we show a linear plot of capture probability *vs* Z. The difference between the rate for Hg and for Pb is well outside the statistical error. Such a difference is to be expected due to the closed-shell properties of the Pb isotopes; the effect is qualitatively discussed by Kennedy, who estimates a dip of about 20 percent, as compared with the 30 percent we observe.

The point for Sb appears to be rather low, and it will be interesting to examine the group of elements in this vicinity. Indeed, while we can say that the capture probability curve is certainly not as regular as was expected according to the Wheeler picture, we have as yet only a sketchy notion of its general character.

A new apparatus is now under construction which will permit us to use much smaller targets. The measurements will then be extended to a larger number of elements.

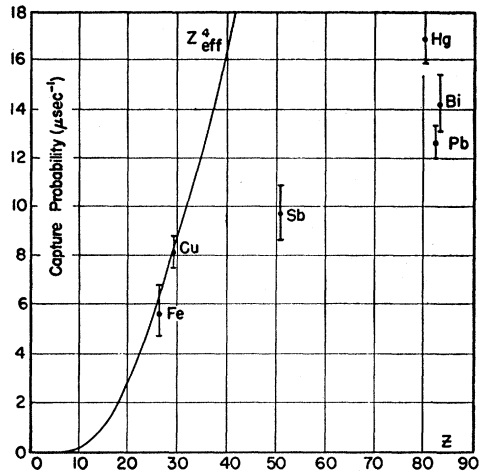

FIG. 10. Capture probabilities *vs* Z, showing especially the discrepancy between Hg and Pb.

Kennedy's calculation of the absorption rate for Pb together with our experimental result gives for the coupling constant between μ-mesons and nucleons the value 3.0×10^{-49} erg cm^3, with an uncertainty of perhaps 25 percent. The strength of this coupling is close to the present values of the beta-decay coupling constant and the constant involved in the spontaneous disintegration of the μ-meson.

A more detailed discussion will be found in Kennedy's paper.

We are indebted to Professor J. A. Wheeler for his continuing interest and stimulating discussions.

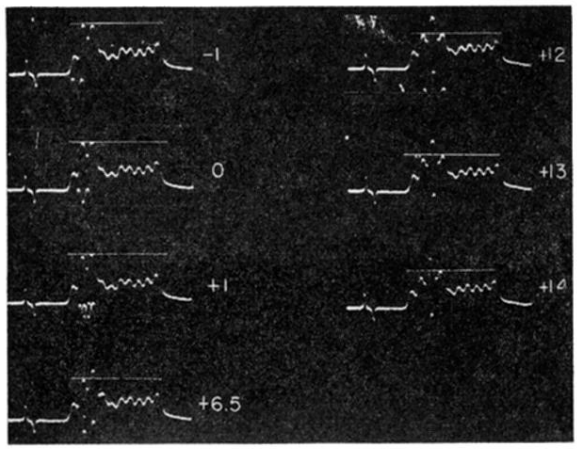

FIG. 5. Photographs of oscilloscope traces obtained using a pair of test pulses from a mercury-switch pulser. The sweep starts after 1.8 μsec. Then, left to right, we have the direct pulse from S_1, delayed 2.6 μsec; the direct S_2, delayed 3.0 μsec; and the chronotron superposition locus, with first detector pulse delayed 4.7 μsec. On the trace labeled "0" the test pulses met on the chronotron line midway between the second and third detectors, since the second and third detector pulses are up, and are just equal. The numbers opposite the other traces indicate the number of feet of Rg-7-U cable inserted between the pulse and the S_2 input of the chronotron; 1 ft = 1.225 mμsec. The zero setting of the chronotron can be shifted at will, of course, by inserting cable in one side.